miR-939 acts as tumor suppressor by modulating JUNB transcriptional activity in pediatric anaplastic large cell lymphoma

Anna Garbin,[1,2] Federica Lovisa,[1,2] Antony B. Holmes,[3] Carlotta C. Damanti,[1,2] Ilaria Gallingani,[1,2] Elisa Carraro,[1] Benedetta Accordi,[1,2] Giulia Veltri,[1,2] Marco Pizzi,[4] Emanuele S.G. d'Amore,[5] Marta Pillon,[1] Alessandra Biffi,[1,2,6] Katia Basso,[3,7] and Lara Mussolin[1,2]

[1]Division of Pediatric Hematology, Oncology and Stem Cell Transplant, Department of Women and Child Health, University of Padua, Padua, Italy; [2]Istituto di Ricerca Pediatrica Città della Speranza, Padova, Italy; [3]Institute for Cancer Genetics, Columbia University, New York, NY, USA; [4]Surgical Pathology and Cytopathology Unit, Department of Medicine, University of Padova, Padova, Italy; [5]Department of Pathological Anatomy, San Bortolo Hospital, Vicenza, Italy; [6]Gene Therapy Program, Dana Farber/Boston Children's Cancer and Blood Disorders Center, Boston, MA, USA and [7]Department of Pathology and Cell Biology, Columbia University, New York, NY, USA

Correspondence: LARA MUSSOLIN - lara.mussolin@unipd.it

doi:10.3324/haematol.2019.241307

miR-939 acts as tumor suppressor by modulating JUNB transcriptional activity in pediatric Anaplastic Large Cell Lymphoma

Anna Garbin, Federica Lovisa, Antony B. Holmes, Carlotta C. Damanti, Ilaria Gallingani, Elisa Carraro, Benedetta Accordi, Giulia Veltri, Marco Pizzi, Emanuele S.G. d'Amore, Marta Pillon, Alessandra Biffi, Katia Basso, Lara Mussolin

Supplementary Material

Patients and cases selection

The laboratory where the present study was carried out is the national reference laboratory for the centralized molecular diagnosis of pediatric non-Hodgkin lymphomas enrolled in the "Associazione Italiana di Ematologia e Oncologia Pediatrica" (AIEOP) treatment protocols. For this reason, systematic collection of the biological material has been initiated several years ago and continues prospectively. The ALCL tumor tissues included in this study were the exceeding material from the diagnostic specimens obtained from 49 pediatric patients affected by *de novo* ALCL, collected in the last 15 years. Formalin-fixed paraffin-embedded tumour biopsies from all the ALCL cases were analyzed by immunohistochemistry using a wide panel of antibodies recognizing T-lineage and B-lineage markers (CD2, CD3, CD4, CD5, CD7, CD8, CD20, CD43, CD45RO, CD79a), NK markers (CD56, CD57), Alk-1, epithelial membrane antigen (EMA) and CD30. In all cases, histologic and immunohistochemical diagnoses were centrally reviewed. All patients were treated according to the international ALCL99 protocol (Brugières *et al*., J Clin Oncol 2009). The percentage of malignant cells in each biopsy specimen was assessed using ALK staining. Diagnosis of ALCL was based on morphological and immunophenotypic criteria, as described in the WHO classification (Swerdlow SH *et al.*, Blood 2016). Malignant cell infiltration was higher than 50% in all tumor tissues analyzed. All patients coexpressed CD30 and EMA. Nuclear and cytoplasmatic expression of ALK was detectable in all the tumour biopsies. Twenty-six patients were classified as common type, 22 with morphological variants, while for 6 cases morphological pattern was not available. The study was approved by ethics committee or by the internal review board of each participating institution and informed consent was obtained from parents or legal guardians before patient enrollment.

Microarray analysis

miRNA expression profiles were generated using the Human microRNA Microarray v.2 (Agilent Techonologies). Raw data were processed with the Feature Extraction Software 9.5.3.1 (Agilent Techonologies), following the manufacturer's indications. The Genes@Work software platform was used for the supervised analysis. The pattern discovery method maps the expression of a

phenotype group of samples (p) onto a control group using an estimate of the cumulative probability density over the control samples. The statistical significance of differential expression of individual miRNAs across the phenotype was assessed using the formula below:

$$z_g = \frac{\mu_p - \mu_c}{\sigma_p - \sigma_c}$$

where μ_p and σ_p are respectively the mean and standard deviation computed for the phenotype group and μ_c and σ_c are respectively the mean and standard deviation computed for the control group. z_g represents the differential expression between the phenotype (p) and control (c) groups relative to the variability of their expression levels. The absolute value of z_g indicates the significance of the differential expression (higher is more significant) and the sign whether the phenotype is up- (positive z_g) or down-regulated (negative z_g) relative to the control.

qRT-PCR for miRNA or mRNA detection

Total RNA was isolated using Trizol Reagent (Life Technologies, ThermoFisher Scientific) following the manufacturer's instruction. Validation of differentially expressed miRNA was performed using TaqMan® MicroRNA Assay (Applied Biosystem, ThermoFisher Scientific). Briefly, 10 ng of total RNA were reverse transcribed and qRT-PCR was set up with TaqMan® Universal PCR Master Mix No Amperase® UNG (Life Technologies). To quantify mRNA levels, 1 µg of total RNA was retrotranscribed with SuperScript II reverse transcriptase (Life Technologies), random hexamers and TaqMan® Universal PCR Master Mix (Applied Biosystem). *NPM-ALK* copies were quantified as previously reported (Pomari *et al.*, Leukemia 2017).

For PDGFRB, TaqMan™ Gene Expression Assay ID 4331182 (Applied Biosystems) and TaqMan™ Fast Advanced Master Mix (Applied Biosystems) were used, whereas TaqMan™ Gene Expression Assay ID 002182 (Applied Biosystems) was used for hsa-miR-939. JUNB primers were previously published (Bladh LG *et al.*, Mol Pharmacol 2005; probe: ACGACTCATACACAGCTACGGGATACGGC). The relative expression levels were calculated according to the comparative delta Ct method, using *ABL1* (Mussolin *et al.*, Leukemia 2014) or hsa-miR-16 (ID 000391, Applied Biosystem) as endogenous controls for mRNAs or miRNA expression respectively. Data were expressed as fold change of reactive lymph nodes (n=11).

Immunoblotting and immunoprecipitation analysis

For immunoblotting and immunoprecipitation, samples were lysed in Triton X-100 sample buffer (50 mM Tris-HCl; 2 mM EDTA; 0.1% SDS; 1% Triton X-100; 1 mM PMSF; 20 µg/ml leupeptin; 20 µg/ml aprotinin; 1:100 phosphatase inhibitor cocktails 2 and 3, Sigma-Aldrich). Protein

concentration was measured by BCA protein assay (ThermoFisher Scientific). For Western blotting analysis, an equal amount of protein (30 µg) were resolved by SDS-PAGE prior to be transferred onto nitrocellulose membrane (PerkinElmer). Blocked membranes were probed for JUNB (mouse, 1:1000, Santa Cruz Biotechnology, Inc.), JUN (rabbit 60A8 #9165, 1:1000, Cell Signaling Technology), using γ-tubulin (mouse, 1:4000, Sigma-Aldrich) as gel loading control. Membranes were incubated with peroxidase-labeled sheep anti-mouse/anti-rabbit IgG (1:2000, GE Healthcare) and visualized with ECL Pro chemiluminescent solution (PerkinElmer) and Hyperfilm autoradiography films (GE Healthcare) or digitally acquired by iBright FL1500 system (ThermoFisher Scientific)

To visualize PDGFRB protein, 100 µg of protein lysates were incubated with PDGFRB antibody (rabbit 28E1 #3169, 1:50, Cell Signaling Technology) at 4°C overnight, and 30 µl of Protein G-Sepharose beads were added to immunocomplexes to for 2 h at 4°C. The immunoadsorbed pellets were washed 4 times with Triton X-100 sample buffer and heated at 95°C in 1X reducing Laemmli loading buffer. Immunoprecipitates were then fractionated by 8% SDS-PAGE and transferred to nitrocellulose membranes for Western blotting analysis. Levels of expressed PDGFRB in the immunoprecipitates were normalized on γ-tubulin (mouse, 1:4000, Sigma-Aldrich) expression obtained by Western blotting using 100 µg of input lysates.

Cell culture

Human ALCL ALK+ cell lines Karpas299 and SUP-M2 were maintained in RPMI 1640 medium containing 10% heat-inactivated fetal calf serum, 2 mmol/l glutamine, 100 U/ml penicillin and 100 µg/ml streptomycin at 37°C in 5% CO_2 in a humidified incubator. All reagents were purchased from Life Technologies (ThermoFisher Scientific).

Transient transfection of pre-miRNA or anti-miRNA

Pre-miRNA negative control (AM17110), pre-miRNA precursor (PM12517) and inhibitor (AM17000) hsa-miR-939 were purchased from Ambion (Life Technologies). Karpas299 cells were transiently transfected with 50 nM of pre-miR-939/control or miR-939 inhibitor/control using *Trans*IT-X2® Transfection Reagent (Mirus Bio), following the manufacturer's instruction. Cells were harvested 24, 48 and 72 hours after transfection and miR-939 expression was assessed by qRT-PCR.

Luciferase reporter assay

The 3'-UTR region of the predicted miR-939 target gene JUNB was amplified from human genomic DNA and cloned into the pmirGLO Dual-Luciferase miRNA Target Expression Vector (Promega). In order to assess the binding of miR-939 to the 3'-UTR sequence of JUNB, Karpas299 and SUP-M2 cells were co-transfected with 50 nM of pre-miR-939 and 50 ng of reporter construct containing wild-type or mutant JUNB 3'-UTR. Lysates were collected 24 hours after transfection and Firefly and Renilla Luciferase activities were measured with a Dual-Luciferase Reporter System (Promega). The 3'-UTR construct was mutagenized at the miR-939 binding site using the Phusion Site-Directed mutagenesis kit (ThermoFisher Scientific), following the manufacturer's instructions. Relative luciferase activity was calculated by normalizing the ratio of Firefly/Renilla luciferase to negative control-transfected cells. Transfections were performed in triplicate.

Migration and clonogenic assay

Migration was tested using cell culture inserts (Transwell) with a 5 μm pore size membrane (24-well format, Corning). The lower compartment contained 0.4 ml of serum-free RPMI medium 0,1% BSA conditioned by 100 ng CXCL12 (Peprotech) as a chemoattractant. Karpas299 or SUP-M2 cells ($1x10^5$) were previously transfected with 50 nM of pre-miR-939, anti-miR-939 or negative control. After 24 hours, cells were resuspended in 650 µl of RPMI medium 0,1% BSA and 200 µl were seeded in the upper compartment in triplicate and placed at 37°C in a humidified incubator with a 5% CO_2 atmosphere. After an incubation of 4 hours, the cells on the lower surface were counted by flow cytometry. For clonogenic assay, Karpas299 and SUP-M2 cells were transfected with negative control, mimic or inhibitor then 500 cells were seeded in MethoCult™ H4230 medium (STEMCELL™) and incubated for 10 days. Numbers of colonies were counted using the image processing program ImageJ (LOCI, University of Wisconsin).

Reverse Phase Protein Arrays (RPPA)

ALCL cells were lysed in an appropriate lysis buffer with proteases and phosphatases inhibitors. Protein lysates were loaded into a 384-well plate, serially diluted with dilution buffer into four-point dilution curves (from undiluted to 1:8) and printed in duplicate on nitrocellulose-coated glass slides (ONCYTE® AVID™ nitrocellulose film slides, Grace Bio-Labs) using the 2470 Arrayer (Aushon BioSystems). Selected slides were stained with FAST GREEN FCF 0.01% (Sigma-Aldrich) a fluorescent dye used to estimate the total protein amount for each printed sample and scanned by ScanArray 4000 (Packard Biochip Technologies). Before antibody staining, slides were blocked in blocking solution (I-Block 2% - Applied BioSystems, 0.1% Tween20 – Sigma-Aldrich - in PBS

1X) for 3 hours at room temperature. Then, blocked slides were stained with antibody (PDGFRB, rabbit 1:75, Cell Signaling Technology) on an automatic slide stainer (Dako Autostaines Plus, Dako Cytomation) using the CSA kit (Dako Cytomation). The TIF images of antibody and Fast Green FCF stained slides were analyzed using MicroVigeneTM software (VigeneTech Inc) and the protein expression signal was quantified for each sample. Briefly, the signal of the negative control array (secondary antibody only) was subtracted from the antibody slide signal and the resulting value was normalized to the total protein content.

Statistical analysis

Data analyses were carried out by using GraphPad Prism 7.0. The t-test was used to determine differences in miR-939 and PDGFRB expression between the groups, migratory and clonogenic potential and luciferase activity. P-value less than 0.05 was considered statistically significant. All P-values are two-sided, with a type I error rate fixed at 0.05. Descriptive statistic was used to define population.

Supplementary Table S1. Clinical and biological characteristics of the 16 pediatric ALCL patients evaluated by microarray analysis

Clinical and biological characteristics		ALK-low expression N=5	ALK-high expression N=11
Gender	Female	1	7
	Male	4	4
Median age at diagnosis (yrs)	≤ 9.6	1	7
	> 9.6	4	4
Stage at diagnosis	I-II	1	1
	III-IV	4	10
CNS involvement	Yes	0	1
	No	5	10
Event	Yes	1	4
	No	4	7
Histological subtypes (2 mv)	Common	3	8
	Other*	1	3

*Other: other than common subtype; mv: missing values

Supplementary Table S2. MicroRNAs significantly deregulated between ALK-low and ALK-high subgroups

Systematic Name	*ALK-low group mean*	*ALK-high group mean*	*FDR*	*Z-score*
hsa-miR-939	7.638	6.731	0.001	1.095
hsa-miR-572	7.159	5.251	0.003	1.058
hsa-miR-638	9.952	8.138	0.007	0.992
hsa-miR-671-5p	5.824	3.990	0.004	0.955
hsa-miR-768-5p	6.960	5.074	0.004	0.914
hsa-miR-923	15.203	12.971	0.011	0.911
hsa-miR-574-5p	7.249	6.233	0.004	0.909
hsa-miR-1224-5p	6.009	4.861	0.009	0.814
hsa-miR-483-5p	6.702	4.959	0.011	0.794
hsa-miR-100	7.660	6.021	0.021	0.734
hsa-miR-338-3p	5.915	5.136	0.016	0.734
hsa-miR-155	8.116	6.982	0.026	0.717
hsa-miR-575	8.749	7.190	0.029	0.698
hsa-miR-188-5p	6.697	5.335	0.047	0.698
hsa-miR-497	8.367	7.211	0.037	0.674
hsa-miR-125a-3p	6.618	5.744	0.027	0.665
hsa-miR-801	7.911	6.676	0.048	0.663
hsa-miR-146a	8.468	7.342	0.037	0.618
hsa-miR-99b	5.466	4.786	0.043	0.594

Supplementary Table S3. Clinical and biological characteristics of the validation cohort

Clinical and biological characteristics		**miR-939 low expression N=25**	**miR-939 high expression N=24**
Gender	Female	9	11
	Male	16	13
Median age at diagnosis (yrs)	≤ 9.9	15	10
	> 9.9	10	14
Stage at diagnosis	I-II	6	4
	III-IV	19	20
CNS involvement	Yes	2	1
	No	23	23
ALK expression	Low	4	6
	High	21	18
Histological subtypes (6 mv)	Common	11	14
	Lymphoistiocitic	5	3
	Small cell	1	-
	Mixed (classic+small cells)	3	3
	Mixed (lymphoistiocitic+ small cell)	2	-
	Hodgkin	-	1
Event	Yes	9°	7°°
	No	16§	17§§

CNS: central nervous system; mv: missing values; ° early relapses (5/9), °° (2/7); short follow-up § (3/16), §§ (3/17).

Supplementary Figure S1. miR-939 levels in Karpas299 and SUP-M2 cells after transient transfection with miR-939 mimic, inhibitor or negative control (NC)

miR-939 expression levels in transfected ALCL cell lines were assessed by qRT-PCR, using the comparative delta Ct method and miR-16 as endogenous control. In cells transfected with miR-939 mimic, expression increased up to 56.6 times in Karpas299 and 137.3 in SUP-M2.

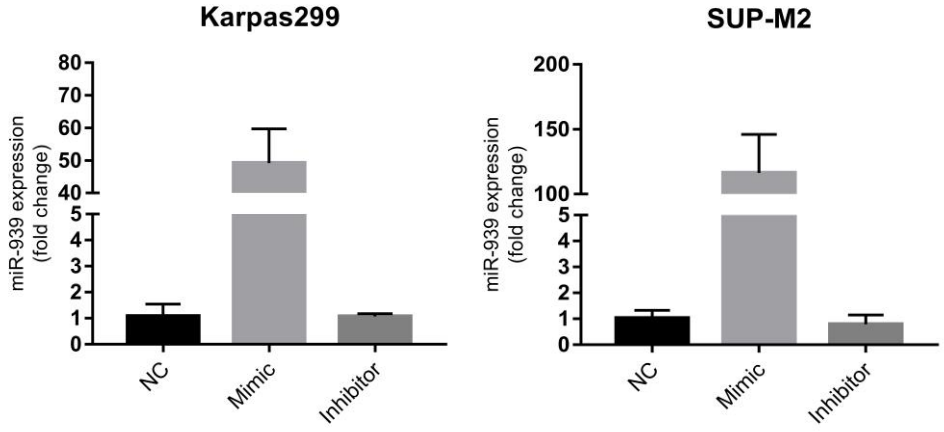

Supplementary Figure S2. *NPM-ALK* expression in Karpas299 and SUP-M2 cell lines after transfection with miR-939 mimic and inhibitor

NPM-ALK mRNA absolute quantification was performed 24 hours after transfection using *ABL* as housekeeping gene. For the generation of the standard curves, plasmids containing *NPM-ALK* and *ABL1* were used. The normalized copy numbers were expressed as copy numbers of *NPM-ALK* per 10^4 copies *ABL1* (ns: P>0.05).

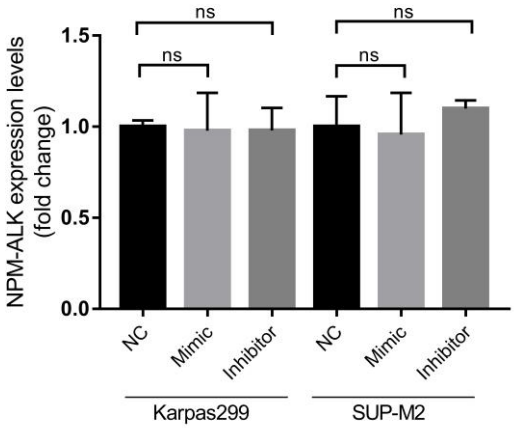

Supplementary Figure S3. *PDGFRB* mRNA expression in Karpas299 and SUP-M2 cells after transfection with miR-939 mimic or negative control

Data have been measured by qRT-PCR according to the comparative delta Ct method and compared to negative controls (NC). miR-16 was used as endogenous control (*P<0.05, ns: P>0.05).

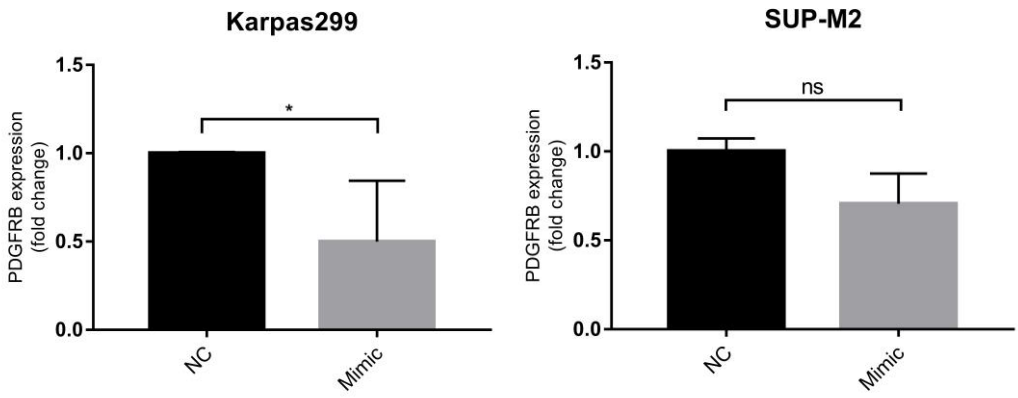

Supplementary Figure S4. *JUNB* mRNA expression levels in ALK-low/-high patients. Expression levels of *JUNB* in 49 ALCL cases. Data have been measured by qRT-PCR according to the comparative delta Ct method and compared to reactive lymph nodes tissue (LN, n=11). *JUNB* median expression level=0.714 (ns: P>0.05).